SPH-LES MODEL FOR WAVE DISSIPATION USING A CURTAIN WALL

Hitoshi GOTOH[1], Songdong SHAO[2] and Tetsu MEMITA[3]

[1]Member of JSCE, Dr. Eng., Associate Professor, Dept. of Civil Eng., Kyoto University
(Yoshida Hon-machi, Sakyo-ku, Kyoto, 606-8501, Japan)
[2]Member of JSCE, Dr. Eng., JSPS Postdoctoral Fellow, Dept. of Civil Eng., Kyoto University
(Yoshida Hon-machi, Sakyo-ku, Kyoto, 606-8501, Japan)
[3]Member of JSCE, Dr. Eng., Senior Research Officer, Tech. Res. Center, The Kansai Electric Power Co. Inc.
(11-20 Nakoji, 3-Chome, Amagasaki, Hyogo, 661-0974, Japan)

The transmission and reflection of regular waves by a half immersed curtain wall is studied by measuring the transmitted and reflected wave histories in the experiment. The experiment investigations were conducted for three different wave heights H = 0.06, 0.07 and 0.08 m with a period of 1.5 s in a wave flume of 50.0 m long, 1.0 m wide and in a constant water depth of 0.72 m. The curtain wall is set on a 1/100 slope with the immersion depth of 0.1 m. The Smoothed Particle Hydrodynamics (SPH) model is employed to reproduce the experimental wave profiles and velocities. The turbulence was dealt with by incorporating a Large Eddy Simulation (LES) model into the numerical code.

Key Words: *regular wave, curtain wall, SPH, LES*

1. INTRODUCTION

Dissipation of wave height and energy from propagating water waves is one of the basic necessities in coastal engineering. Different types of wave breakwaters have been designed throughout the world for this purpose. Among them a partially immersed curtain-type breakwater, which is a rigid vertical wall ascending from a fraction of the water depth to upwards, has many advantages. Since most of the wave energy is concentrated within near the surface, this curtain wall can effectively defend coastal areas. Meanwhile, water circulation is maintained in the gap below and it has no negative effects on the marine scenery and will never create a dead water zone for marine life. Thus the wall itself is actively for altering the flow rather than passively resisting wave actions as a conventional breakwater does.

The importance of this issue had been early addressed by Ursell[1)] and Wiegel[2)] using analytical approaches based on the potential theory. Recently further improvement has been made by Lo[3)] in his eigenfunction approach incorporating the flexibility of the wall membrane. With regard to experimental work, Reddy and Neelaman[4)] carried out a detailed experiment using a wide range of wave steepness and different immersion depths of the barrier to study the wave transmission and reflection processes.

The experiment conducted in this study is better in that the curtain wall is situated on a sloping bottom rather than a flat one. The setting is more practical, considering the fact that most real breakwaters are built on the shallow water region where the local topography has a sloping angle. The numerical model employed here is based on the SPH, or the solver of the Navier-Stokes equations, which are capable of providing full details of flow in the area of interest. As compared with existing grid methods, the SPH model is much more effective in describing free surfaces by particles without numerical diffusion. The wave transmission and reflection characteristics are studied based on the comparison between the experimental data and numerical computations. In addition, the computed turbulence eddy viscosity and velocity distributions are also shown to demonstrate the robustness of the incorporated LES sub-particle scale turbulence model. The findings will provide useful information

on the design of future breakwaters, suggesting that turbulence production is the main cause of water wave dissipation.

2. NUMERICAL MODELS

Here the Smoothed Particle Hydrodynamics (SPH) is employed to solve the basic hydrodynamic equations. It originated in astrophysics for the study of fluid dynamics of interstellar gas and has later been extended to model a wide range of hydrodynamics problems by Monaghan[5]. The basic concept is that the dependent field variables can be expressed exactly by integrals which are approximated by summation interpolants over neighboring particles. From this, spatial derivatives are similarly evaluated by summation interpolants. Thus each term in the Navier-Stokes equations, including the density, pressure gradient, divergence and viscosity (or Laplacian) can be represented by SPH formulations. Combining with suitable initial and boundary conditions, the whole equation is solvable. The robustness of the SPH lies in its easy and accurate free surface tracking by Lagrangian particles with no additional numerical diffusions as usually encountered in the grid method. Meanwhile, a Large Eddy Simulation (LES) Smagorinsky[6] model is incorporated into the SPH code for addressing possible turbulence at the sub-particle scale, the concept of which is the same as the SPS-turbulence model by Gotoh et al.[7].

The governing equations for SPH-LES model are the mass and momentum conservation equations written in Lagrange form as

$$\frac{1}{\rho}\frac{D\rho}{Dt}+\frac{\partial u_i}{\partial x_i}=0 \tag{1}$$

$$\frac{Du_i}{Dt}=-\frac{1}{\rho}\frac{\partial P}{\partial x_i}+g_i+2\frac{\partial}{\partial x_j}[(\nu_0+\nu_t)S_{ij}] \tag{2}$$

where ρ = fluid density; t = time; u_i = velocity; P = pressure; g_i = external force; ν_0 = laminar kinematic viscosity; and ν_t = turbulence eddy viscosity, which is determined by the well-known Smagorinsky[6]

$$\nu_t=(C_s\Delta)^2|S| \tag{3}$$

where C_s = Smagorinsky constant (0.1); Δ = particle spacing; and $|S|$ = local strain rate given by

$$|S|=(2S_{ij}S_{ij})^{1/2} \tag{4}$$

$$S_{ij}=\frac{1}{2}\left(\frac{\partial u_i}{\partial x_j}+\frac{\partial u_j}{\partial x_i}\right) \tag{5}$$

The SPH computation consists of two steps, i.e. prediction and correction, similar to those employed in the Moving Particle Semi-implicit (MPS) method by Koshizuka, Nobe and Oka[8], and Gotoh and Sakai[9]. The prediction step is an explicit integration of the stress tensor, viscous and gravitational terms in Equation (2) in time sequence without enforcing incompressibility. The second correction step updates intermediate field values using the pressure obtained from the Poisson equation by enforcing incompressibility.

3. EXPERIMENTS

(1) Experimental settings

The experiment was conducted at a wave flume of 50.0 m long, 1.0 m wide and 1.2 m deep in the Technical Research Center, The Kansai Electric Power Company Incorporated. The curtain wall was located at x = 0.0 m on a 1/100 uniform slope. The non-reflecting wave paddle was located offshore side at x =-31.2 m, producing an incident wave with a period of T = 1.5 s and over a constant water depth of D = 0.72 m. The local water depth at the curtain wall was 0.2 m and the height of opening beneath the curtain wall was 0.1 m. Three different wave heights H = 0.06, 0.07 and 0.08 m were employed in the experiment under conditions of non-overtopping and overtopping of the curtain wall. A schematic view of the experimental settings and measurement sections are shown in Fig. 1.

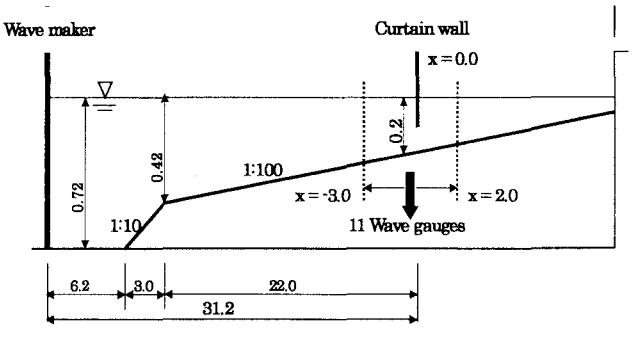

Fig. 1 Schematic view of experimental settings

(2) Experimental results

The following results correspond to the non-overtopping experiment in which the incident wave height is H = 0.08 m. The time series of measured wave heights at the point most far from the

wave paddle (at $x = 2.0$ m), is shown in Fig. 2. It is seen that about 33.0 s or 22 wave periods after the initiation of the wave paddle, the quasi-steady status can be achieved. A video picture near the curtain wall taken within one wave period T is given in Fig. 3, from which the complete processes of the wave incoming, reflecting and transmitting are shown.

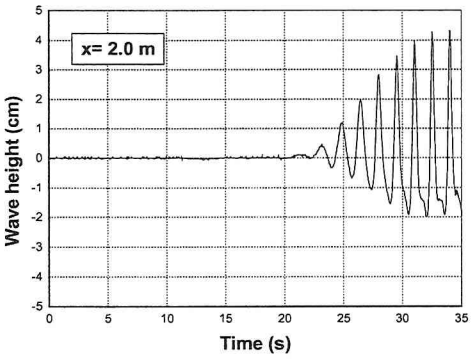

Fig. 2 Time series of transmitted wave height at $x = 2.0$ m

(3) Experimental analysis

The time sequences of wave profiles at three key positions x=-2.0, 0.0, 2.0 m are shown in Fig. 4(a), (b), and (c), respectively. The figures include the experimental data covering two wave periods from t=34.0 s to 37.0 s. It is shown from Fig. 4(a) that the wave height on the offshore side of the curtain wall is significantly higher than the incident wave height H = 0.08 m. This is due to the interference and superposition of incoming and reflecting waves, which causes unfavorable flow conditions. The wave profile at the curtain wall in Fig. 4(b) is relatively stable and symmetric about the still water line. The wave height is about 65% of the deep-water value and the wave dissipation effect is obvious. However, significant wave deformation is observed on the onshore side at Fig. 4(c), where the amplitude of the wave crest is two times higher than that of the corresponding wave trough. Two possible reasons would contribute to this characteristics. Firstly, the transmitted wave under the curtain wall is composed of different phases and easily decomposes during subsequent propagation. Secondly, as the transmitted wave further travels towards the onshore side, it gradually enters the shallow water region in which the wave becomes more and more unstable and tends to be breaking. In addition, Fig. 4 clearly indicates that at all locations the wave period almost maintains a constant value of 1.5 s, which is equal to the deep water value. This is also consistent with the theoretical analysis that the wave period does not change during its shoaling processes.

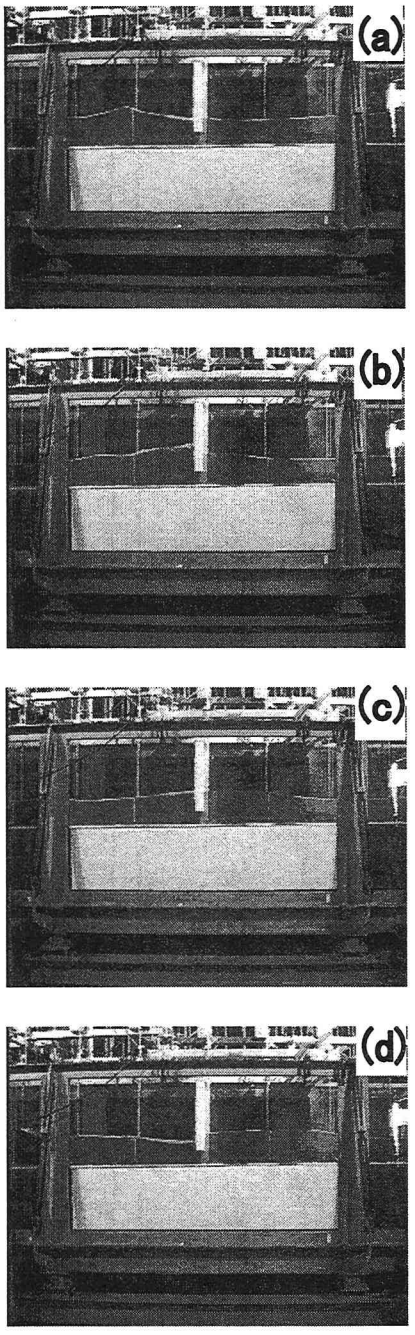

Fig. 3 Wave profile recordings near curtain wall. (a) $t/T = 0.0$; (b) $t/T = 0.25$; (c) $t/T = 0.50$; and (d) $t/T = 0.75$

4. NUMERICAL COMPUTATION

(1) Computational settings

The SPH is employed to reproduce the above experimental results. The computational domain is taken to be 6.0 m long, covering $x = \pm 3.0$ m. The incident wave is created by moving a numerical wave paddle on the offshore boundary. The time step is automatically adjusted in the computation to satisfy the stability conditions of Courant constraint and viscous diffusion. The possible turbulence

effects during the wave transmission and reflection are evaluated by the incorporated LES sub-particle scale model. The initial particle spacing is 0.01 m and approximately 12,000 particles are employed in the computation.

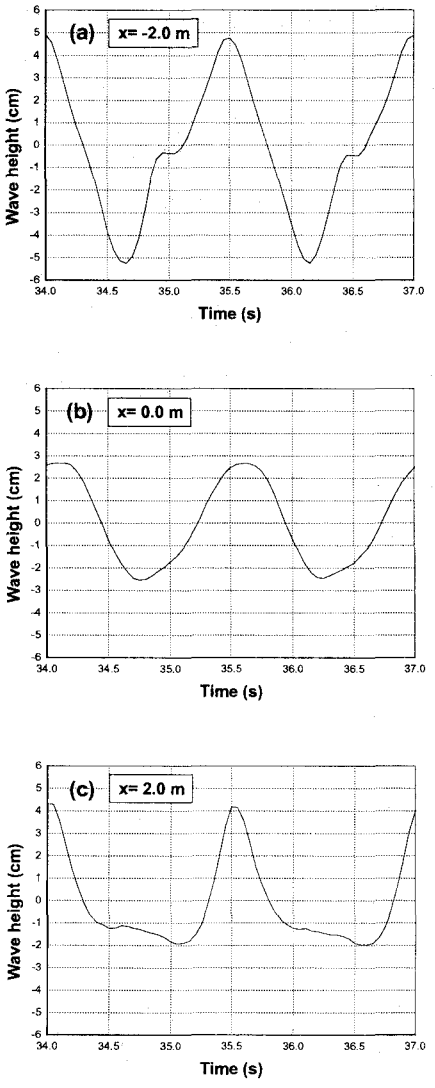

Fig. 4 Time series of wave height at three representative locations. (a) x = -2.0 m; (b) x = 0.0 m; and (c) x = 2.0 m

(2) Computational results and analysis

The instantaneous particle configurations during one wave period near the curtain wall within $x = \pm 1.0$ m are given in Fig. 5 (a) ~ (d), in which the curtain wall is located at x = 0.0 m with the thickness of 5.0 cm. By being compared with corresponding experimental snapshots in Fig. 3, it is shown that the computations reproduce the experiment very well in view of both the wave shape and wave amplitude. In order to quantitatively evaluate the accuracy of the SPH computations, the computed wave surface profiles during single wave period are plotted against experimental data in Fig. 6 (a) ~ (d). The agreement is quite satisfactory and the maximum discrepancy is within the order of 1.0 cm.

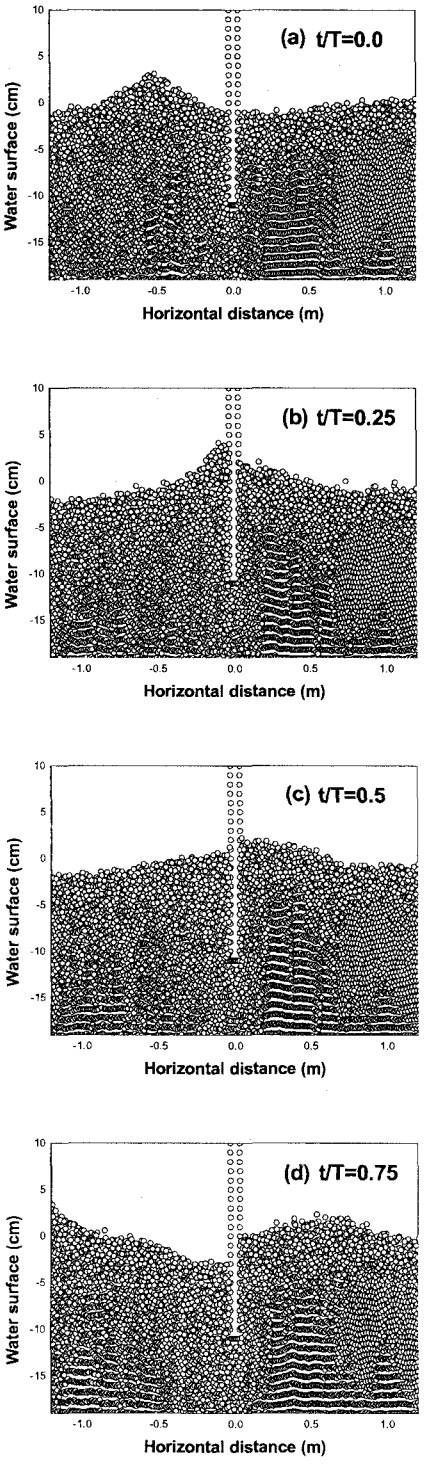

Fig. 5 Particle configurations of wave transmission and reflection processes. (a) t/T = 0.0; (b) t/T = 0.25; (c) t/T = 0.50; and (d) t/T = 0.75

Thus the reliability of the SPH with the incorporated LES sub-particle scale turbulence model is verified.

Furthermore, the turbulence eddy viscosity and velocity distributions are given in Fig. 7 (a) and (b) to show the robustness of the turbulence modeling.

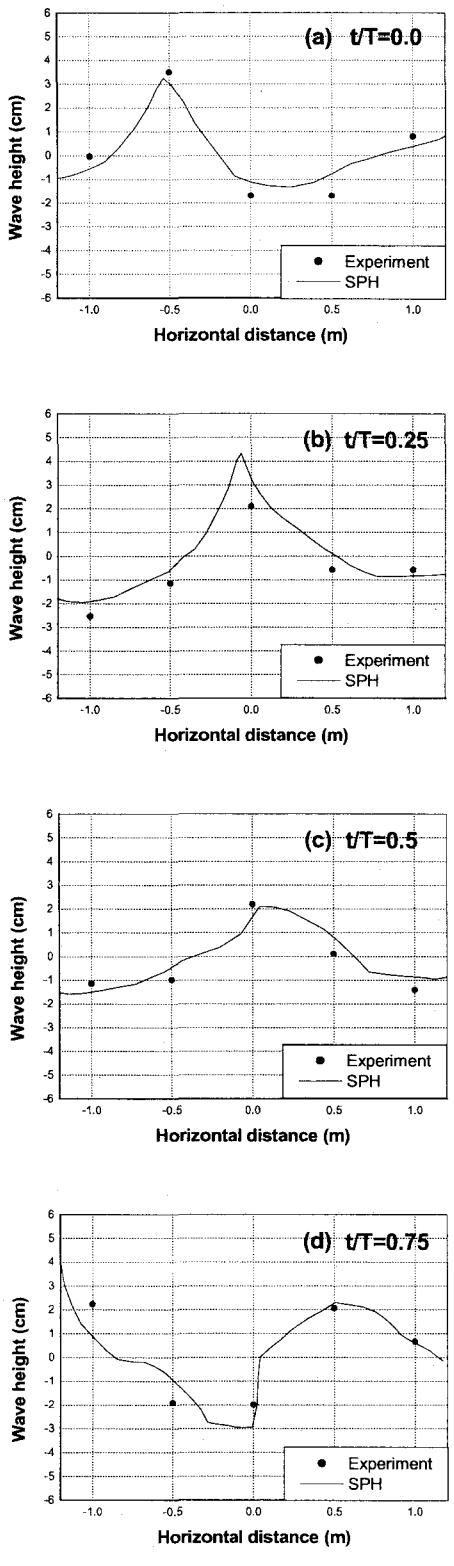

Fig. 6 Comparisons between experimental and computational wave profiles near the curtain wall. (a) t/T = 0.0; (b) t/T = 0.25; (c) t/T = 0.50; and (d) t/T = 0.75

It is seen from Fig. 6 that during single wave period the wave profiles deform significantly during propagation processes. The maximum wave deformation occurs when the wave trough approaches the curtain wall at $t/T = 0.75$ in Fig. 6 (d), where the trough surface becomes extremely flat. This characteristic is mainly caused by the interactions between the incoming and reflecting waves, as well as subsequent rundown motion. Thus it can be concluded that the offshore region just in the vicinity of the curtain wall is frequently subjected to unfavorable flow conditions and should be paid great attention in practice. Besides, it is also noted that there exists an abrupt water surface drop at the location of the wall, which further contributes to unfavorable flow conditions nearby.

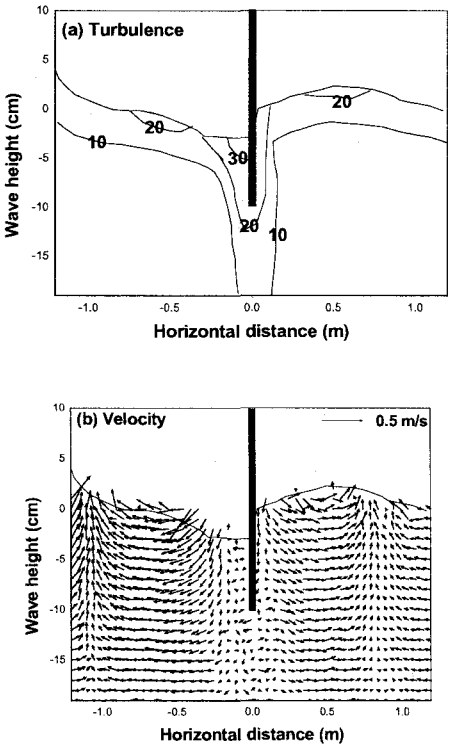

Fig.7 Computational results at time t/T = 0.75. (a) Turbulence eddy viscosity ν_t/ν_0; and (b) Velocity field

It is well known that turbulence is the main source of energy dissipation. One quantitative measurement of turbulence intensity is the turbulence energy k. If we assume local energy equilibrium condition of the sub-particle turbulence, k can be related to the turbulence eddy viscosity ν_t by a constant (Gotoh et al. 2001). In Fig.7 (a) the turbulence eddy viscosity is given at time t/T = 0.75, the values of which

have been normalized by laminar viscosity ν_0 of 10^{-6} m^2/s. It is seen that the turbulence sources mainly concentrate near the flow surface and around the curtain wall. The maximum eddy viscosity is 30 times that of the laminar value, occurring at the interface between the fluid and curtain wall on the offshore side. Here a backwash is created by the rundown motion. The velocity field in Fig.7 (b) further suggests that the velocity under the curtain wall is very complicated and weak circulation can be roughly seen. However, the velocity distributions become quite orderly in the region away from the wall, consistent with classical water wave theory[10].

Although no experimental data have been available for comparison, the robustness of the incorporated LES turbulence model is fully understood by the reproduction of small eddies around and under the curtain wall as shown in Fig. 7 (b). Without the use of LES model, eddies of the particle scale can only be dealt with, while eddies of the sub-particle scale are very difficult to be detected. The LES model also gives out reasonable turbulence intensity distributions as show in Fig. 7 (a), supporting the accuracy of water surface computations. Some other traditional turbulence models such as $k \sim \varepsilon$ model or Reynolds equation, usually overestimate turbulence intensity by several orders when applied to wave hydrodynamics, although they have been very mature in river engineering applications. In addition, the current LES turbulence model is fairly easy for programming.

5. CONCLUSION

The paper presents a SPH-LES model to study regular wave reflection and transmission processes by a half immersed curtain wall. The model is effective in tracking free surfaces by particles and dealing with turbulence by the incorporated sub-particle scale turbulence model.

Both the experimental and numerical results demonstrate that over half of the incident wave energy can be blocked by the curtain wall. However, the transmitted wave will become unstable as it propagates further towards onshore during shoaling processes. The offshore region just in front of the curtain wall is frequently subjected to interactions of incoming and reflecting waves, leading to unfavorable flow conditions. It is also noted that there exists an abrupt water surface drop at the location of the wall, which further contributes to the complicity of flow conditions nearby. In addition, the computed turbulence eddy viscosity and velocity distributions suggest that the main cause of water wave dissipation is due to the production of the turbulence during the wave running down and reflecting processes.

ACKNOWLEDGEMENT: This research work was supported by the Japan Society for the Promotion of Science. In addition, the valuable comments from Professor Tetsuo Sakai, Department of Civil Engineering, Kyoto University, are highly appreciated. We are also very grateful to Mr. Tetsuo Yagi, master course student of Department of Civil Engineering, Kyoto University, for his work on experimental data processing.

REFERENCES

1) Ursell, F.: The effect of a fixed vertical barrier in surface waves in deep water, *Proc. Cambridge Phil. Soc.*, Vol. 43, No. 3, pp. 374-382, 1947.
2) Wiegel, R. L.: Transmission of wave past a rigid vertical thin barrier", *J. Waterway and Harbors Div.*, ASCE, Vol. 86, No. WW1, pp. 1-12, 1960.
3) Lo, Y. M. Edmond: Performance of a flexible membrane wave barrier of a finite vertical extent, *Coastal Eng. J.*, JSCE, Vol. 42, No. 2, pp. 237-251, 2000.
4) Reddy, M. S. and Neelaman S.: Wave transmission and reflection characteristics of a partially immersed rigid vertical barrier, *Ocean Engineering*, Vol. 19, No. 3, pp. 313-325, 1992.
5) Monaghan, J. J.: Smoothed particle hydrodynamics, *Annu. Rev. Astron. Astrophys.*, Vol. 30, pp. 543-574, 1992.
6) Smagorinsky, J.: General circulation experiments with the primitive equations, I. The basic experiment, *Mon. Weath. Rev.*, Vol. 91, pp. 99-164, 1963.
7) Gotoh, H., Shibahara, T. and Sakai, T.: Sub-particle-scale turbulence model for the MPS method–Lagrangian flow model for hydraulic engineering, *Comp. Fluid Dynamics. J*, Vol. 9, No. 4, pp. 339-347, 2001.
8) Koshizuka S., Nobe, A. and Oka, Y.: Numerical analysis of breaking waves using the moving particle semi-implicit method, *Int. J. Numer. Meth. Fluids*, Vol. 26, pp. 751-769, 1998.
9) Gotoh, H. and Sakai, T.: Lagrangian simulation of breaking waves using particle method, *Coastal Eng. J.*, JSCE, Vol. 41, No. 3&4, pp. 303-326, 1999.
10) Dean, R. G. and Dalrymple, R. A.: Water Wave Mechanics for Engineers and Scientists, *Adv. Series Ocean Eng.*, Vol. 2, World Scientific, pp. 295-325, 1991.

(Received September 30, 2002)